

Experimental determination of flexoelectric coefficients in SrTiO₃, KTaO₃, TiO₂, and YAlO₃ single crystals

Christopher A. Mizzi , Binghao Guo , and Laurence D. Marks *

Department of Materials Science and Engineering, Northwestern University, Evanston, Illinois 60208, USA

 (Received 5 February 2022; accepted 11 April 2022; published 23 May 2022)

We report experimental values for the flexoelectric responses of SrTiO₃, KTaO₃, TiO₂, and YAlO₃ single crystals using a three-point bending approach. We find all samples possess a linear flexoelectric response with effective short-circuit flexoelectric coefficients $\sim |1-10|$ nC/m. Flexocoupling voltages computed from these measured effective flexoelectric coefficients are found to significantly vary across the investigated materials and refute the previous suggestions that they should be $\sim |1-10|$ V. Importantly, we find that low dielectric constant materials can have large flexocoupling voltages exceeding nominal expectations.

DOI: [10.1103/PhysRevMaterials.6.055005](https://doi.org/10.1103/PhysRevMaterials.6.055005)

I. INTRODUCTION

The first experimental report of the flexoelectric effect in crystalline solids is attributed to Bursian and Zaikovskii who, in 1968, observed that BaTiO₃ thin films tended to bend when exposed to electric fields [1]. Their work provided direct confirmation of a coupling between strain gradient and polarization, i.e., flexoelectricity, which had been predicted by Mashkevich and Tolpygo [2]. For the ensuing 33 years, flexoelectricity would go largely unnoticed in the solid-state community until a series of experiments by Ma and Cross [3–7] demonstrated its importance in high dielectric constant ceramics, beginning a revival of interest in flexoelectricity.

Significant experimental and theoretical progress on the flexoelectric effect in the past 20 years is evidenced by the dramatic increase in the number of papers exploring the phenomenon in crystalline solids [8,9]. Much of this interest has been driven by the relevance of the flexoelectric effect at the nanoscale: because of the intrinsic scaling of strain gradient with size, large flexoelectric responses occur at small length scales, even for materials with modest flexoelectric properties [10–13]. For example, there are reports of flexoelectric polarizations comparable with spontaneous ferroelectric polarizations near crack tips [14] and dislocations [15]. Another major driving force behind the interest in flexoelectricity is that the effect imbues all insulators with an electromechanical functionality similar to piezoelectricity, which is only intrinsic in a subset of materials without inversion symmetry [16]. Beyond the fundamental science of flexoelectricity, there are indications of promising applications in energy harvesting [17,18], strain sensing [19], and actuation [20], and the links between flexoelectricity, biology [21–24], and triboelectricity [25–27] suggest potential medical and industrial relevance.

The flexoelectric response of a material is governed by a fourth-rank tensor. Under the short-circuit boundary conditions commonly employed in experiments, the linear coupling

between polarization (P_i) and strain gradient ($\epsilon_{kl,j} = \frac{\partial \epsilon_{kl}}{\partial x_j}$) is described by short-circuit flexoelectric coefficients (μ_{ijkl}) defined as

$$\mu_{ijkl} = \left. \frac{\partial P_i}{\partial \epsilon_{kl,j}} \right|_{E=0}. \quad (1)$$

While short-circuit flexoelectric coefficients are a convenient experimental measure of the strength of flexoelectric couplings, flexocoupling voltages are a more fundamental measure of this strength because they directly enter free energy expansions as the coefficient of the flexoelectric contribution [8,9]. Flexocoupling voltages (f_{ijkl}) are related to short-circuit flexoelectric coefficients through

$$\mu_{ijkl} = \epsilon_0 \chi f_{ijkl}, \quad (2)$$

where ϵ_0 is the permittivity of free space and χ is dielectric susceptibility [8,9]; they define the strain-gradient-induced electric field.

The first attempts to quantify flexocoupling voltages were estimates made in 1964 by Kogan [28], which indicated $f \sim |1-10|$ V. More sophisticated treatments based on stability analyses led to similar predictions: upper bounds for *intrinsic* flexocoupling voltages (i.e., not including contributions from defects or the mean-inner potential) should be $\sim |1-10|$ V [29–32]. While this predicted flexocoupling voltage range is supported by *ab initio* calculations [32–35] and some experiments [36], it has not been extensively tested. Furthermore, if flexocoupling voltages do exhibit little variation across materials as predicted, then it follows from Eq. (2) that short-circuit flexoelectric coefficients should scale linearly with dielectric susceptibility.

However, the scarcity of flexoelectric coefficient measurements on high-quality single crystals has limited a detailed comparison between experiment and theory. Early work by Ma and Cross [3–7] focused on technologically relevant ceramics, but it is known that material defects can also have a large effect [15,37–39]. In addition, it is much easier to measure the magnitude of these coefficients. Determining their

*L-marks@northwestern.edu

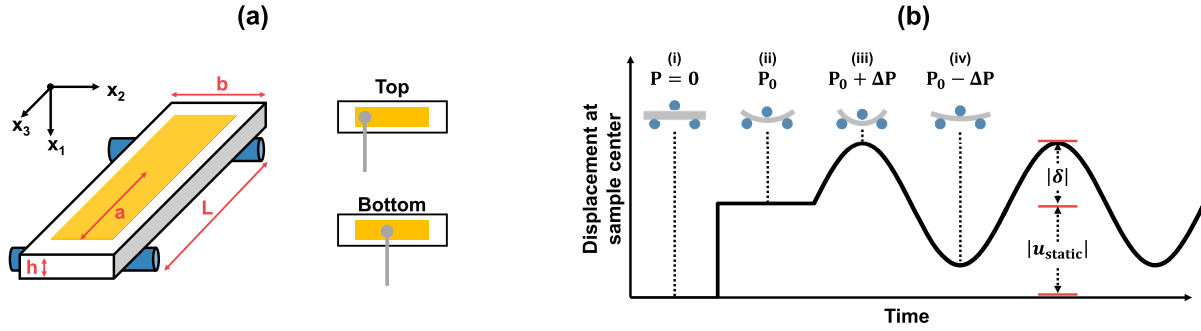


FIG. 1. (a) A typical sample used for flexoelectric characterization has a width of b , thickness of h , and sits on supports (blue) spaced L apart. Electrodes (yellow) with half-length a are deposited on the sample, and then leads (gray) are attached to the electrodes with silver paste. Throughout this paper, x_1 and x_3 refer to the primary bending axis and long axis of the sample, respectively. (b) Summary of three-point bending flexoelectric characterization. (i) An initially unpolarized sample (gray) resting on three-point bending supports (blue) is subjected to (ii) a static displacement at the sample center (u_{static}) which bends the sample and induces a static polarization P_0 . An oscillatory displacement (δ) (iii) increases and (iv) decreases P_0 by an amount ΔP . δ is proportional to the strain gradient [Eq. (4)], and the short-circuit current is proportional to ΔP [Eq. (5)].

sign is experimentally more subtle. To advance the field, there is a need to increase the database of experimental values, particularly to test *ab initio* methods on more complex crystal structures than have been studied to date.

In this paper, we characterize the flexoelectric responses of SrTiO₃, KTaO₃, TiO₂, and YAlO₃ single crystals using a three-point bending approach. Linear flexoelectric responses with effective short-circuit flexoelectric coefficients $\sim |1-10|$ nC/m are found in all samples. The corresponding flexocoupling voltages vary significantly and thus refute the previous suggestions that they should be $\sim |1-10|$ V. Our results also demonstrate that low dielectric constant materials can have flexocoupling voltages exceeding nominal expectations.

II. METHODS

A. Sample preparation

Single crystals ($10 \times 10 \times 0.5$ mm) purchased from MTI Corporation were diced into beams ($10 \times 3 \times 0.5$ mm) using a TechCut 5 Precision Sectioning Machine (Allied High Tech Products, Inc.) with a diamond wafering blade. After solvent cleaning, the crystals were baked in a tube furnace at 600°C for 6 h in air to minimize surface contamination. Gold electrodes ($8 \times 2 \times 50$ nm) were deposited on the top and bottom surfaces of the beams using a shadow mask in a Denton DESK III sputter coater. Silver paste (SPI Silver Paste Plus) was used to attach wire leads to the electrodes. Finally, the samples were baked in a tube furnace at 300°C for 2 h in air to improve the electrical conductivity and the mechanical stability of the contacts.

B. Flexoelectric characterization

Flexoelectric characterization was performed using the three-point bending approach described by Zubko *et al.* [36]. An oscillatory strain gradient was applied to a sample in a three-point bending configuration with a dynamical mechanical analyzer (TA Instruments RSA-III) while a lock-in amplifier (Signal Recovery 7265 Dual Phase DSP) measured the short-circuit current generated in response to the applied

strain gradient through the flexoelectric effect. Figure 1 provides a summary of the three-point bending approach to flexoelectric characterization and illustrates a typical sample with definitions of the sample dimensions and axes convention used throughout this paper. Note, the axes x_1 , x_2 , and x_3 are abbreviated below with the subscripts 1, 2, and 3.

In the three-point bending geometry, the flexoelectric response of the sample is characterized by an effective flexoelectric coefficient, defined as

$$\bar{P}_1 = \mu_{\text{eff}} \bar{\epsilon}_{33,1}, \quad (3)$$

where μ_{eff} describes the average polarization generated through the sample thickness (\bar{P}_1) owing to the transverse strain gradient applied to the sample averaged over the electrode area ($\bar{\epsilon}_{33,1}$). Within the limits of Euler-Bernoulli beam theory [40], the average transverse strain gradient over the electrode area is given by

$$\bar{\epsilon}_{33,1} = 12 \frac{L-a}{L^3} \delta, \quad (4)$$

where L is the spacing between the three-point bending supports, a is the electrode half-length, and δ is the measured displacement in the x_1 direction at the beam center. \bar{P}_1 is related to the short-circuit current (I) measured through the electrodes via

$$\bar{P}_1 = \frac{I}{2A\omega}, \quad (5)$$

where A is the electrode area, and ω is the radial frequency of the strain gradient applied with the dynamical mechanical analyzer. The magnitude of μ_{eff} is found by computing the slope of \bar{P}_1 as a function of $\bar{\epsilon}_{33,1}$. The sign of μ_{eff} is deduced from the phase difference between \bar{P}_1 and $\bar{\epsilon}_{33,1}$: a positive (negative) μ_{eff} corresponds to an in-phase (out-of-phase) relationship between \bar{P}_1 and $\bar{\epsilon}_{33,1}$ [41].

The μ_{eff} measured in this type of experiment is a linear combination of flexoelectric tensor components and elastic constants [36]. The exact form of this linear combination depends on sample orientation, crystallography, and the extent to which anticyclic bending is suppressed. For example, Zubko *et al.* [36] showed that, in the pure beam-bending limit, a cubic

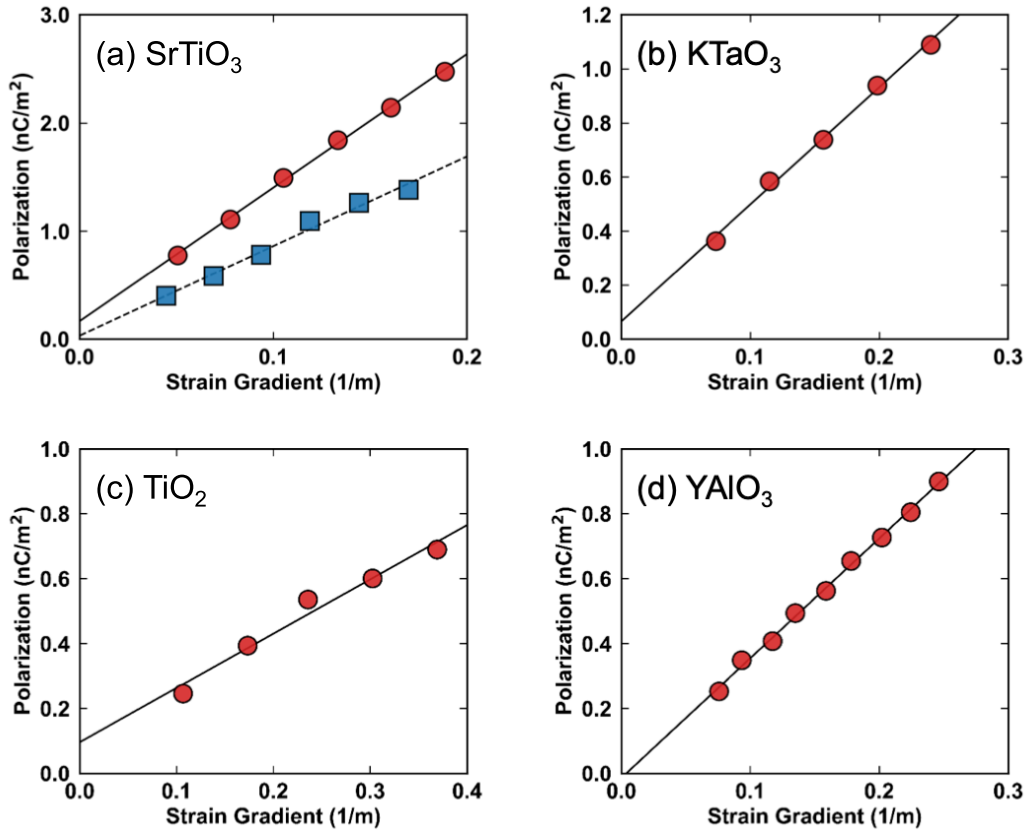


FIG. 2. Flexoelectric characterization of an array of commercially available single crystals. All samples exhibit a linear flexoelectric response [$r^2 > 0.98$ with root mean square error < 0.05 for each fit] with effective flexoelectric coefficients $\sim |1-10|$ nC/m, determined from the slope of \bar{P}_1 as a function of $\bar{\epsilon}_{33,1}$. In each plot, lines are least squares fits to the measured data (circles and squares). The size of the data points is indicative of the uncertainty in each measurement. For (a), red circles and blue squares correspond to SrTiO₃ samples with $x_1 \parallel [100]$ and $[110]$, respectively. Orientations and effective flexoelectric coefficients for each sample are given in Table I.

sample with $\langle 100 \rangle$ -type edges has

$$\mu_{\text{eff}} = (1 - \nu) \mu_{1122} - \nu \mu_{1111}, \quad (6)$$

where ν is Poisson's ratio.

III. RESULTS

The materials studied here (SrTiO₃, KTaO₃, TiO₂, and YAIO₃) are undoped, wide bandgap insulators commercially available as high-quality single crystals. The latter detail is important to minimize extrinsic contributions to the flexoelectric response of the samples originating from defects (which are known to enhance flexoelectric responses [15,37–39]) so that intrinsic flexoelectric properties can be isolated. These materials represent a series of archetypal structures: the cubic perovskite (SrTiO₃, KTaO₃), rutile (TiO₂), and orthorhombic perovskite (YAIO₃) structures. Each of these structures contains similarly coordinated sublattices with differences in site symmetries, making these measurements a useful standard for future first-principles calculations. While experimental flexoelectric coefficients have been previously reported for SrTiO₃ [20,36,42,43] and TiO₂ [38,44] single crystals, we have chosen to explore flexoelectricity in these two systems to both benchmark our apparatus and confirm the reported values of the effective flexoelectric coefficients since there are indications of significant sample-to-sample variations [36].

Figure 2 shows representative measurements of the effective flexoelectric coefficients on SrTiO₃, KTaO₃, TiO₂, and YAIO₃ samples. All measured flexoelectric responses are found to be highly linear, independent of composition, point group, or crystallographic orientation. The effective flexoelectric coefficients with errors corresponding to 95% confidence intervals of least squares fits are given in Table I. They are $\sim 1-10$ nC/m across all measured samples, although the signs differ depending on the sample orientation and material: the SrTiO₃ sample with $[110] \parallel x_1$ and the YAIO₃ sample both had negative effective flexoelectric coefficients. For reference, the table also includes values for DyScO₃ and LaAlO₃, measured using the same experimental setup, which have been previously reported in Refs. [11,37], respectively.

The effective flexoelectric coefficients of SrTiO₃ included in Table I are in good agreement with literature values, even matching the sign change observed by Zubko *et al.* [36] for $[100]$ - vs $[110]$ -oriented crystals. These measurements are also comparable with measurements of flexoelectric coefficients in SrTiO₃ using the inverse method [20]. Other measurements of flexoelectric coefficients have been performed on thin SrTiO₃ samples [42,43], but these methods appear to yield substantially larger flexoelectric coefficients.

The measured value of the effective flexoelectric coefficient for TiO₂ agrees with literature measurements of $\sim 1-10$ nC/m, though a direct comparison with existing

TABLE I. Material, point group, crystallographic orientation, effective flexoelectric coefficient, dielectric susceptibility, and effective flexocoupling voltage for each of the samples measured in this paper. Uncertainties correspond to the 95% confidence interval of the least squares fits shown in Fig. 2. The axes for YAlO_3 and DyScO_3 refer to the $Pnma$ setting. Pseudocubic (pc) axes are used for LaAlO_3 . Data for DyScO_3 and LaAlO_3 are taken from Refs. [11,37], respectively. The dielectric susceptibilities are taken from Refs. [45–50].

Material	Point group	x_1	x_2	x_3	μ_{eff} (nC/m)	χ	f_{eff} (V)
SrTiO_3	$m3m$	[100]	[010]	[001]	$+12.4 \pm 0.6$	369	$+3.8 \pm 0.2$
SrTiO_3	$m3m$	[110]	$[\bar{1}10]$	[001]	-8.3 ± 1.4	369	-2.5 ± 0.4
KTaO_3	$m3m$	[100]	[010]	[001]	$+4.4 \pm 0.5$	241	$+2.1 \pm 0.2$
TiO_2	$4/mmm$	[100]	[010]	[001]	$+1.7 \pm 0.3$	85	$+2.3 \pm 0.6$
YAlO_3	mmm	[101]	$[10\bar{1}]$	[010]	-3.7 ± 0.2	15	-28 ± 1.5
DyScO_3	mmm	[101]	$[10\bar{1}]$	[010]	-8.4 ± 0.4	23	-42 ± 2.0
LaAlO_3	$\bar{3}m$	$[100]_{\text{pc}}$	$[010]_{\text{pc}}$	$[001]_{\text{pc}}$	$+3.2 \pm 0.3$	24	$+15 \pm 1.4$

measurements is difficult because (1) the reported flexoelectric coefficient for single-crystal TiO_2 measured with three-point bending did not report crystallographic orientation [38], and (2) the other measurement in the literature was performed on polycrystalline thin films using a cantilever based approach [44]. In both cases, it is not possible to deduce the functional form of the effective flexoelectric coefficient.

The cubic perovskite KTaO_3 yields an effective flexoelectric coefficient comparable with other cubic perovskites such as SrTiO_3 [36] and pseudocubic perovskites like LaAlO_3 [37]. Similarly, the magnitude and sign of the effective flexoelectric coefficient of YAlO_3 are like the magnitude and sign of the effective flexoelectric coefficient obtained on isostructural DyScO_3 samples with the same crystallographic orientation [11].

The effective flexoelectric coefficients and literature values for the dielectric susceptibility [45–50] in Table I can be used to calculate the effective flexocoupling voltages for each of the samples measured in this paper using Eq. (2). Figure 3(a) shows the flexocoupling voltage magnitudes averaged over all samples and crystallographic orientations for a particular materials system as a function of dielectric constant. We limit our analysis in Fig. 3 to these samples since they have all been prepared in the same manner, and flexoelectric responses are thought to have significant sample-to-sample variation, likely stemming from defects [15,37–39] or mean-inner potential contributions [51,52]. Our measure-

ments indicate that flexocoupling voltages (1) do not appear to be structurally insensitive and (2) exhibit substantially larger variation than effective short-circuit flexoelectric coefficients, which are $\sim |1-10| \text{ nC/m}$ across the measured materials and do not linearly scale with dielectric constant [Fig. 3(b)]. We find that low dielectric constant oxides possess flexocoupling voltages $\sim 5-10\times$ larger than the flexocoupling voltages of high dielectric constant oxides.

While we are unable to invert the three-point bending measurements to obtain individual flexoelectric tensor components [36], it is possible to estimate the magnitude of the intrinsic contributions to the effective flexocoupling voltage, which can be calculated from first principles [33–35,53,54], using the Ibers approximation to the mean-inner potential [55], as described in Ref. [51]. We use experimental lattice parameters [50,56–59], atomic electron scattering factors from Ref. [60], and assume a Poisson’s ratio of 0.24 to compute f_{MIP} . This approximation is accurate to $\sim 20\%$ [51]. Table II displays the values of f_{MIP} and $f_{\text{intrinsic}}$, the mean-inner potential and intrinsic contributions to the measured f_{eff} , respectively. Here, $f_{\text{intrinsic}}$ are also shown as a function of dielectric constant in Fig. 3(c). The values in Table II provide a point of direct comparison for first-principles predictions of flexoelectric coefficients. We find $f_{\text{MIP}} \sim +10 \text{ V}$ in all cases and $f_{\text{intrinsic}}$ negative in most cases, the latter in agreement with the density functional theory calculations of Hong and Vanderbilt [34]. The sign of $f_{\text{intrinsic}}$ for LaAlO_3 is within the

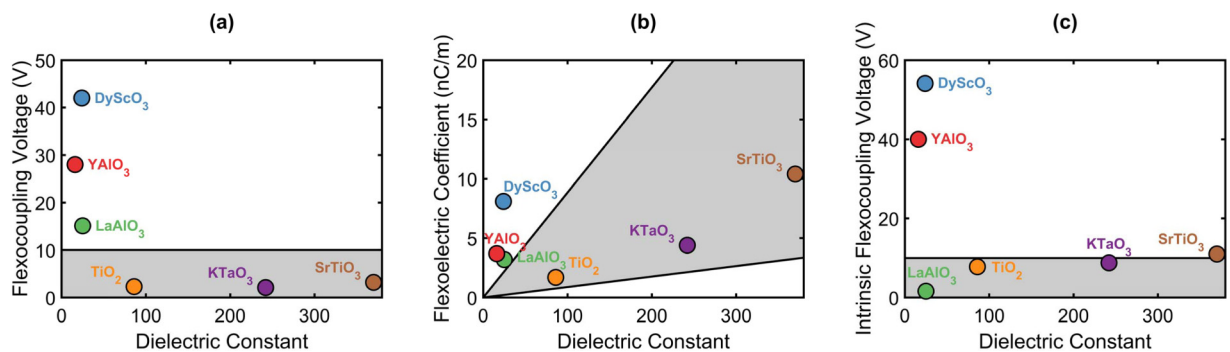


FIG. 3. The average magnitudes of the (a) effective flexocoupling voltage, (b) effective flexoelectric coefficient, and (c) intrinsic contribution to the flexocoupling voltage as a function of dielectric constant for each single-crystal oxide reported here or measured with the same technique in previous investigations (see Refs. [11,37]). Shaded regions correspond to theoretical ranges based upon phenomenological predictions.

TABLE II. Decomposition of measured effective flexocoupling voltages (f_{eff}) into mean-inner potential (f_{MIP}) and intrinsic contributions ($f_{\text{intrinsic}}$) according to Ref. [51]. Effective flexoelectric coefficients measured in LaAlO_3 and DyScO_3 are taken from Refs. [37,11], respectively.

Material	f_{eff} (V)	f_{MIP} (V)	$f_{\text{intrinsic}}$ (V)
SrTiO_3 (100)	$+3.8 \pm 0.2$	+11.6	-7.8
SrTiO_3 (110)	-2.5 ± 0.4	+11.6	-14
KTaO_3	$+2.1 \pm 0.2$	+10.9	-8.8
TiO_2	$+2.3 \pm 0.6$	+10.1	-7.8
YAlO_3	-28 ± 1.5	+12.0	-40
DyScO_3	-42 ± 2.0	+12.1	-54
LaAlO_3	$+15 \pm 1.4$	+13.5	+1.6

uncertainty of the approximations. As with the measured effective flexocoupling voltages, the magnitude of the effective $f_{\text{intrinsic}}$ for YAlO_3 and DyScO_3 exceeds the phenomenological estimate of $|1-10|$ V.

IV. DISCUSSION

The measurements reported above on a wide range of single-crystal oxides indicate short-circuit flexoelectric coefficients are essentially constant, with values $\sim |1-10|$ nC/m in all the investigated materials. By contrast, the flexocoupling voltages show substantial variation, with lower dielectric constant oxides possessing flexocoupling voltages which exceed phenomenological estimates [8,9,28,29,61]. Since all the mean-inner potential contributions to the measured effective flexocoupling voltages [51] are approximately +10 V, the variation in the flexocoupling voltage throughout these materials originates from intrinsic contributions. It is worth noting that counting arguments do not account for the differences in the magnitude of the intrinsic flexocoupling voltage: if the large flexocoupling voltages in DyScO_3 and YAlO_3 were a consequence of the effective flexoelectric coefficient expression measured in three-point bending having contributions from additional flexoelectric tensor components, then both the flexoelectric coefficients and flexocoupling voltages should be anomalously large.

The question is then: Why are the flexocoupling voltages so large in several compounds? The first-principles theory of flexoelectricity [34,35] suggests a possible explanation: reduced site-symmetry [34]. Hong and Vanderbilt [34] demonstrated that flexoelectric coefficients can be expressed

as charge density and force responses to long-wavelength phonon perturbations. In this framework, a flexoelectric coefficient is the sum of three terms: (1) a purely electronic term present in materials of any symmetry, (2) a lattice-dipole term consisting of contributions from infrared-active zone-center modes, and (3) a lattice-quadrupole term corresponding to contributions from Raman-active zone-center modes. Both YAlO_3 and DyScO_3 have distorted orthorhombic structures with space group $Pnma$ at room temperature and atmospheric pressure, characterized by combinations of octahedral rotations and antipolar A-site displacements [58,62]. Cations and anions in this structure have low site symmetries that lead to nontrivial lattice-quadrupole contributions to flexoelectric tensor components (these are zero in higher-symmetry structures such as cubic perovskites); some work in this direction for PbZrO_3 has recently been submitted by Shapovalov and Stengel [63]. YAlO_3 is a particularly good candidate for future first-principles calculations [34] because it does not have the complexity associated with modeling $4f$ electrons, which are present in DyScO_3 (e.g., Ref. [64]). Such first-principles calculations will also be useful to elucidate the relative importance of different structural distortions (e.g., disentangling contributions from octahedral rotations and A-site antipolar displacements) and explore the impact, if any, of proximities to ferroelectric instabilities on flexoelectricity [65].

V. CONCLUSIONS

We have measured the flexoelectric response in SrTiO_3 , KTaO_3 , TiO_2 , and YAlO_3 single crystals using a three-point bending approach. Our measurements indicate short-circuit flexoelectric coefficients are essentially constant in these materials, with values $\sim |1-10|$ nC/m. These effective flexoelectric coefficients correspond to flexocoupling voltages which show significant structural sensitivity and exceed phenomenological predictions. An analysis of the mean-inner potential contributions to the measured flexocoupling voltages suggests the anomalously large flexocoupling voltages are an intrinsic phenomenon. These findings provide important benchmarks for future calculations of flexoelectricity.

ACKNOWLEDGMENTS

This paper was supported by the U.S. Department of Energy, Office of Science, Basic Energy Sciences, under Award No. DE-FG02-01ER45945. C.A.M. performed flexoelectric characterization and analysis. C.A.M. and B.G. performed sample preparation. All work was supervised by L.D.M. All authors contributed to the writing of the paper.

- [1] E. V. Bursian and O. I. Zaikovskii, *Sov. Phys. Solid State* **10**, 1121 (1968).
 [2] V. Mashkevich and K. Tolpygo, *Sov. Phys. JETP* **5**, 435 (1957).
 [3] W. Ma and L. E. Cross, *Appl. Phys. Lett.* **78**, 2920 (2001).
 [4] W. Ma and L. E. Cross, *Appl. Phys. Lett.* **81**, 3440 (2002).
 [5] W. Ma and L. E. Cross, *Appl. Phys. Lett.* **82**, 3293 (2003).
 [6] W. Ma and L. E. Cross, *Appl. Phys. Lett.* **86**, 072905 (2005).

- [7] W. Ma and L. E. Cross, *Appl. Phys. Lett.* **88**, 232902 (2006).
 [8] P. Zubko, G. Catalan, and A. K. Tagantsev, *Annu. Rev. Mater. Res.* **43**, 387 (2013).
 [9] P. V. Yudin and A. K. Tagantsev, *Nanotechnology* **24**, 432001 (2013).
 [10] G. Catalan, A. Lubk, A. H. G. Vlooswijk, E. Snoeck, C. Magen, A. Janssens, G. Rispens, G. Rijnders, D. H. A. Blank, and B. Noheda, *Nat. Mater.* **10**, 963 (2011).

- [11] P. Koirala, C. A. Mizzi, and L. D. Marks, *Nano Lett.* **18**, 3850 (2018).
- [12] D. Lee, A. Yoon, S. Y. Jang, J. G. Yoon, J. S. Chung, M. Kim, J. F. Scott, and T. W. Noh, *Phys. Rev. Lett.* **107**, 057602 (2011).
- [13] T. D. Nguyen, S. Mao, Y.-W. Yeh, P. K. Purohit, and M. C. McAlpine, *Adv. Mater.* **25**, 946 (2013).
- [14] H. Wang, X. Jiang, Y. Wang, R. W. Stark, P. A. van Aken, J. Mannhart, and H. Boschker, *Nano Lett.* **20**, 88 (2020).
- [15] P. Gao, S. Yang, R. Ishikawa, N. Li, B. Feng, A. Kumamoto, N. Shibata, P. Yu, and Y. Ikuhara, *Phys. Rev. Lett.* **120**, 267601 (2018).
- [16] P. S. Halasyamani and K. R. Poeppelmeier, *Chem. Mater.* **10**, 2753 (1998).
- [17] Q. Deng, M. Kammoun, A. Erturk, and P. Sharma, *Int. J. Solids Struct.* **51**, 3218 (2014).
- [18] X. N. Jiang, W. B. Huang, and S. J. Zhang, *Nano Energy* **2**, 1079 (2013).
- [19] W. B. Huang, S. R. Yang, N. Y. Zhang, F. G. Yuan, and X. N. Jiang, *Exp. Mech.* **55**, 313 (2015).
- [20] U. K. Bhaskar, N. Banerjee, A. Abdollahi, Z. Wang, D. G. Schlom, G. Rijnders, and G. Catalan, *Nat. Nanotechnol.* **11**, 263 (2016).
- [21] K. D. Breneman, W. E. Brownell, and R. D. Rabbitt, *PLoS One* **4**, e5201 (2009).
- [22] R. Núñez-Toldrà, F. Vasquez-Sancho, N. Barroca, and G. Catalan, *Sci. Rep.* **10**, 254 (2020).
- [23] A. G. Petrov, *Biochim. Biophys. Acta* **1561**, 1 (2002).
- [24] F. Vasquez-Sancho, A. Abdollahi, D. Damjanovic, and G. Catalan, *Adv. Mater.* **30**, 1705316 (2018).
- [25] C. A. Mizzi, A. Y. W. Lin, and L. D. Marks, *Phys. Rev. Lett.* **123**, 116103 (2019).
- [26] C. A. Mizzi and L. D. Marks, *Nano Lett.* (2022), doi: 10.1021/acs.nanolett.2c00240.
- [27] K. P. Olson, C. A. Mizzi, and L. D. Marks, *Nano Lett.* (2022), doi: 10.1021/acs.nanolett.2c00107.
- [28] S. M. Kogan, *Sov. Phys. Solid State* **5**, 2069 (1964).
- [29] P. V. Yudin, R. Ahluwalia, and A. K. Tagantsev, *Appl. Phys. Lett.* **104**, 082913 (2014).
- [30] E. A. Eliseev, A. N. Morozovska, M. D. Glinchuk, and R. Blinc, *Phys. Rev. B* **79**, 165433 (2009).
- [31] A. N. Morozovska, E. A. Eliseev, C. M. Scherbakov, and Y. M. Vysochanskii, *Phys. Rev. B* **94**, 174112 (2016).
- [32] M. Stengel, *Phys. Rev. B* **93**, 245107 (2016).
- [33] J. Hong and D. Vanderbilt, *Phys. Rev. B* **84**, 180101(R) (2011).
- [34] J. Hong and D. Vanderbilt, *Phys. Rev. B* **88**, 174107 (2013).
- [35] M. Stengel, *Phys. Rev. B* **88**, 174106 (2013).
- [36] P. Zubko, G. Catalan, A. Buckley, P. R. L. Welche, and J. F. Scott, *Phys. Rev. Lett.* **99**, 167601 (2007).
- [37] C. A. Mizzi, B. Guo, and L. D. Marks, *Phys. Rev. Materials* **5**, 064406 (2021).
- [38] J. Narvaez, F. Vasquez-Sancho, and G. Catalan, *Nature (London)* **538**, 219 (2016).
- [39] Z. Wang, C. Li, Z. Zhang, Y. Hu, W. Huang, S. Ke, R.-K. Zheng, F. Li, and L. Shu, *Scr. Mater.* **210**, 114427 (2022).
- [40] L. D. Landau and E. M. Lifshitz, *Theory of Elasticity*, 2nd ed. (Pergamon, New York, 1970).
- [41] J. Narvaez, S. Saremi, J. Hong, M. Stengel, and G. Catalan, *Phys. Rev. Lett.* **115**, 037601 (2015).
- [42] V. Harbola, S. Crossley, S. S. Hong, D. Lu, Y. Birkhölzer, Y. Hikita, and H. Y. Hwang, *Nano Lett.* **21**, 2470 (2021).
- [43] S. Das, B. Wang, T. R. Paudel, S. M. Park, E. Y. Tsymbal, L.-Q. Chen, D. Lee, and T. W. Noh, *Nat. Commun.* **10**, 537 (2019).
- [44] F. J. Maier, M. Schneider, J. Schratzenholzer, M. Artner, K. Hradil, A. Artemenko, A. Kromka, and U. Schmid, *Acta Mater.* **190**, 124 (2020).
- [45] H. E. Weaver, *J. Phys. Chem. Solids* **11**, 274 (1959).
- [46] D. Kahng and S. H. Wemple, *J. Appl. Phys.* **36**, 2925 (1965).
- [47] R. A. Parker, *Phys. Rev.* **124**, 1719 (1961).
- [48] S.-Y. Cho, I.-T. Kim, and K. S. Hong, *J. Mater. Res.* **14**, 114 (1999).
- [49] S. Coh, T. Heeg, J. H. Haeni, M. D. Biegalski, J. Lettieri, L. F. Edge, K. E. O'Brien, M. Bernhagen, P. Reiche, R. Uecker, S. Trolier-McKinstry, D. G. Schlom, and D. Vanderbilt, *Phys. Rev. B* **82**, 064101 (2010).
- [50] S. A. Hayward, F. D. Morrison, S. A. T. Redfern, E. K. H. Salje, J. F. Scott, K. S. Knight, S. Tarantino, A. M. Glazer, V. Shuvaeva, P. Daniel, M. Zhang, and M. A. Carpenter, *Phys. Rev. B* **72**, 054110 (2005).
- [51] C. A. Mizzi and L. D. Marks, *J. Appl. Phys.* **129**, 224102 (2021).
- [52] M. Stengel, *Phys. Rev. B* **90**, 201112(R) (2014).
- [53] C. E. Dreyer, M. Stengel, and D. Vanderbilt, *Phys. Rev. B* **98**, 075153 (2018).
- [54] M. Stengel, *Nat. Commun.* **4**, 2693 (2013).
- [55] J. A. Ibers, *Acta Crystallogr.* **11**, 178 (1958).
- [56] R. Diehl and G. Brandt, *Mater. Res. Bull.* **10**, 85 (1975).
- [57] C. J. Howard, T. M. Sabine, and F. Dickson, *Acta Cryst. B* **47**, 462 (1991).
- [58] M. Schmidbauer, A. Kwasniewski, and J. Schwarzkopf, *Acta Cryst. B* **68**, 8 (2012).
- [59] E. A. Zhurova, Y. Ivanov, V. Zavodnik, and V. Tsirelson, *Acta Cryst. B* **56**, 594 (2000).
- [60] D. Rez, P. Rez, and I. Grant, *Acta Cryst. A* **50**, 481 (1994).
- [61] A. K. Tagantsev, *Phys. Rev. B* **34**, 5883 (1986).
- [62] S. Geller and E. A. Wood, *Acta Cryst.* **9**, 563 (1956).
- [63] K. Shapovalov and M. Stengel, arXiv:2112.12167.
- [64] C. A. Mizzi, P. Koirala, and L. D. Marks, *Phys. Rev. Materials* **2**, 025001 (2018).
- [65] N. A. Benedek and C. J. Fennie, *J. Phys. Chem. C* **117**, 13339 (2013).